

An integrated 8-channel Tx/Rx body coil for 7 Tesla whole-body MRI

Stephan Orzada¹, Andreas K. Bitz², Marcel Gratz^{1,3}, Sören Johst¹, Maximilian N. Völker¹, Oliver Kraff¹, Dominik Beyer¹, Tristan Mathiebe¹, Ashraf Abuelhaija⁴, Klaus Solbach⁴, and Mark E. Ladd²

¹Erwin L. Hahn Institute for MRI, Essen, NRW, Germany, ²Medical Physics in Radiology, German Cancer Research Center (DKFZ), Heidelberg, Germany,

³High-field and Hybrid MR Imaging, University Clinic Essen, Essen, Germany, ⁴RF Technology, University Duisburg-Essen, Duisburg, Germany

Target audience: MR coil designers at ultra-high field

Introduction: At ultra-high field, local Tx/Rx arrays are commonly used for body imaging (1-3). These arrays are often bulky and consume much of the limited space in the bore. This restricts the patient size to those with a fairly slender body physique. To allow patients with a larger body physique and a more clinic-like workflow, an integrated Tx/Rx body coil situated between the gradient coil and the lining of the scanner bore might be an option. In this work we present an 8-channel Tx/Rx array which is situated between the inner bore liner and the gradient coil similar to the body coils in standard low-field systems.

Materials and Methods: All experiments were performed on a Siemens Magnetom 7 T whole-body system equipped with a custom 8-channel RF shimming system. The space between the bore liner and the gradient coil is ca. 34 mm; the complete body array has to fit into this confined space. Figure 1 shows the 8-channel coil array on the bore liner. It consists of 8 microstrip line elements with meanders in a circular arrangement, interconnected with slotted ground planes. Each single element is 25 cm long, 9 cm wide, and 2 cm thick. The distance between the microstrip and the bore liner is 5 mm. The width of the meander structure and therefore the electrical length was reduced from 65 mm (Ref. 2) to 60 mm to compensate for the extra dielectric loading of the bore liner. All elements have fixed tuning and matching. T/R-switches are connected to the central feeding network of the elements via Aircell 5 cables of an appropriate length (ca. 70 cm) to ensure pre-amp decoupling. Detuning of the elements is done with detuning boards containing PIN diodes that produce an RF short circuit of the transmit cable to ground when a forward current is applied. These detuning boards are placed in the transmit chain between the RFPAs and the T/R switches. In addition to allowing detuning of the elements, this placement reduces spurious noise from the RFPAs during reception. The bore liner was clad with vibration dampening material to reduce acoustic noise in the bore; only a small area around the array was excluded.

The reverse voltage and forward current for the PIN diodes are supplied by a 2-channel controller. This controller is placed directly at the back of the magnet. In forward mode it delivers 1.2 A as a current source, whereas it delivers 12 V as a voltage source in reverse mode. Switching between the two states takes 5 μ s. The correct timing and logic for switching are supplied via optical connections from a custom-built control unit outside the scanner room.

A QA protocol consisting of various commonly used sequences, RF noise measurements, and transmit power requirements was used to ensure unaltered conventional operation with local transmit/receive arrays.

Results and discussion: The QA protocol did not reveal any degradation in local Tx/Rx array performance when the integrated body coil is detuned.

Inserting the bore liner with the array was complicated due to the small margin left between the array and the gradient coil. The lowermost element of the array was slightly damaged in the process and therefore had an S_{11} of only -1.8 dB. The fixed matching of the other elements was load-dependent and better than -8 dB under varying loading conditions. The coupling between well matched elements was less than -20 dB for neighboring elements and less than -35 dB between all other elements when loaded with a human volunteer. Figure 2A shows the noise correlation of the integrated array. When comparing the transmit voltages for the integrated array and the flexible body array from Ref. 2 in an oval cylindrical oil phantom, the transmit voltage is 3.3 times higher for the integrated array in a transverse slice in the center of the coils. Figure 2B and 2C show 50 cm coronal field-of-view (FOV) gradient echo images with the two coils. These images demonstrate that the integrated coil has a larger FOV in the z-direction. The SNR in such a central coronal slice is 76% of that of the close-fitting coil, and 62% in a central transverse slice when the mean excitation flip angle in the central transverse slice is the same for both coils.

Figure 3 shows GRAPPA g-factor maps obtained with a pseudo multiple replica method for both arrays in an oil phantom. As expected, the close-fitting array performs better. Figure 4 shows gradient echo images of a male human volunteer (1.74 cm, 80 kg) acquired with the integrated body array. Figure 4A shows a transverse view, Figure 4B shows a coronal view with 50 cm field of view. The images are quite homogeneous over this large FOV.

Conclusion: It is feasible to integrate a 7 T 8-channel body array under the bore liner. While transmit efficiency and SNR are reduced in comparison to a close-fitting array, a larger FOV in the z-direction is available. Better tuning and matching will increase the transmit efficiency. Future work will include the implementation of RF power amplifiers close to the bore, and increasing the channel count of the body coil to 32.

References: 1. Metzger et al. MRM 59:396-409 (2008), 2. Orzada et al. Proc. Int'l. Soc. MRM 2009 #2999, 3. Raaijmakers et al. MRM 66:1488-1497 (2001).

Acknowledgement: The research leading to these results has received funding from the European Research Council under the European Union's Seventh Framework Programme (FP/2007-2013) / ERC Grant Agreement n. 291903 MReXcite.

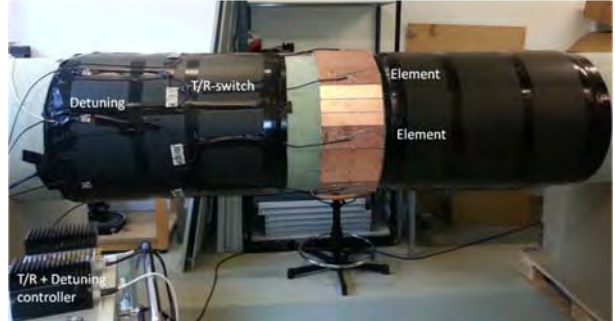


Figure 1: The body array including T/R-switches, detuning boards, and controller.

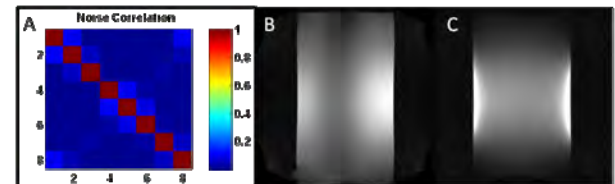


Figure 2: Noise correlation of the integrated array (A). 50 cm coronal FOV acquired with the integrated array (B) and the flexible close-fitting coil (C).

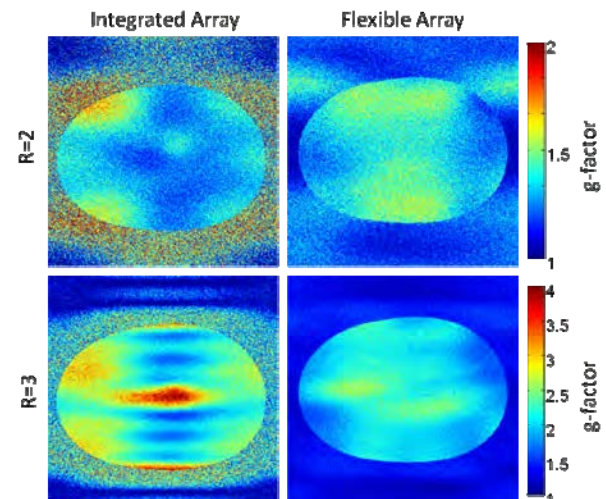


Figure 3: g-factors maps for the integrated body array and the local flexible body array for acceleration factors of 2 and 3.

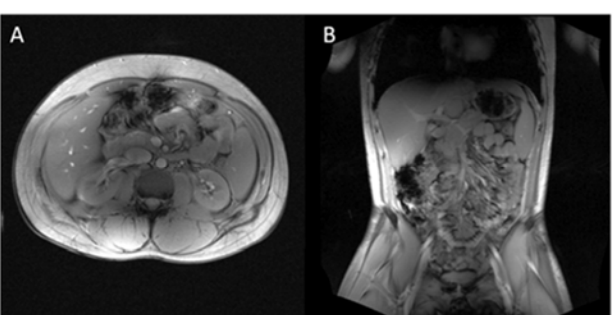


Figure 4: Gradient echo images of a human volunteer acquired with the integrated body array. A) Transverse view, B) Coronal, 50 cm field of view. No intensity correction was applied.